

# Optical Engineering

OpticalEngineering.SPIEDigitalLibrary.org

## **Self-calibrating phase measurement based on diffraction theory and numerical simulation experiments**

Liao Zhou  
Qiu Qi  
Xian Hao

# Self-calibrating phase measurement based on diffraction theory and numerical simulation experiments

Liao Zhou,<sup>a,b,c,d,\*</sup> Qiu Qi,<sup>b</sup> and Xian Hao<sup>a,c</sup>

<sup>a</sup>Chinese Academy of Sciences, The Laboratory on Adaptive Optics, Institute of Optics and Electronics, Chengdu 610209, China

<sup>b</sup>University of Electronic Science and Technology of China, School of Optoelectronic Information, Chengdu 610054, China

<sup>c</sup>Chinese Academy of Sciences, The Key Laboratory on Adaptive Optics, Chengdu 610209, China

<sup>d</sup>University of Chinese Academy of Sciences, Beijing 100049, China

**Abstract.** To achieve a full-aperture, diffraction-limited image, a telescope's segmented primary mirror must be properly phased. Furthermore, it is crucial to detect the piston errors between individual segments with high accuracy. Based on the diffraction imaging theory, the symmetrically shaped aperture with an arbitrarily positioned entrance pupil would focus at the optical axis with a symmetrical diffraction pattern. By selecting a single mirror as a reference mirror and regarding the diffraction image's center as the calibration point, a function can be derived that expresses the relationship between the piston error and the distance from the center of the inference image to the calibration point is linearity within one-half wavelength. These theoretical results are shown to be consistent with the results of a numerical simulation. Using this method, not only the piston error, but also the tip-tilt error can be detected. This method is simple and effective; it yields high-accuracy measurements and requires less computation time. © The Authors. Published by SPIE under a Creative Commons Attribution 3.0 Unported License. Distribution or reproduction of this work in whole or in part requires full attribution of the original publication, including its DOI. [DOI: 10.1117/1.OE.54.2.025116]

Keywords: segmented mirror; piston error; diffractive image; numerical simulation.

Paper 141736 received Nov. 9, 2014; accepted for publication Jan. 30, 2015; published online Feb. 25, 2015.

## 1 Introduction

The segmented primary mirror is one of the best choices for constructing a large telescope. The world's largest telescopes—e.g., Keck, HET, LAMOST, TMT—all adopt segmented primary mirrors. According to this design, the primary mirror is composed of a number of hexagonally shaped aspheric mirrors. Compared with the monolithic primary mirror telescope, the segmented primary mirror must be properly phased in order to achieve a diffraction-limited image. Furthermore, it is crucial to detect piston errors among individual segments with high accuracy. Techniques for detecting the piston error have been developed and successfully used on Keck, HET, JWST, etc.<sup>1,2</sup> These include the narrow-band phasing algorithm,<sup>3</sup> the broadband phasing algorithm,<sup>4</sup> the phase discontinuity sensing (PDS) algorithm, and the dispersed fringe sensing (DFS) algorithm, among others.<sup>5,6</sup> The optical systems of the first two algorithms are comparatively simple though they require more calculation time. On the other hand, the detection accuracies of the last two algorithms are relatively high, but the optical configuration is more complex. Other detecting methods have also been studied.

In this paper, we propose a detecting method—based on the theory of diffraction—that modifies the method for measuring the phase error proposed by Chan et al.<sup>3,7–9</sup> Our method proceeds by selecting one of the segmented mirrors as a reference plane and its diffraction image center as a calibration point; the relation between the piston error (between two adjacent segmented mirrors) and the distance from the center of the interference image to the calibration point can then be derived. When we obtain the interference image center with piston error, the piston error between two adjacent segmented mirrors can then be calculated.

Numerical simulations are carried out, and the results are shown to be consistent with the theoretical calculation results. This detection method is simple, efficient, and highly accurate.

This paper is arranged as follows. First, we deduce an expression for the diffraction image of a rectangular aperture with an arbitrary position for the entrance pupil. Next, we analyze the interference image of two adjacent rectangular apertures with piston error, and deduce the relation between the piston error (between two adjacent segmented mirrors) and the position of the center of the interference image. At last, numerical simulations are carried out in order to verify the theoretical equations.

## 2 Theory

### 2.1 Diffraction Image of a Rectangular Aperture with an Arbitrarily Positioned Entrance Pupil

We select a symmetrically shaped aperture (may be rectangle, circle, and hexagon) at the entrance pupil. We then suppose that the aperture is rectangular (Fig. 1), that the sides are  $2a$  and  $2b$ , that the center is located at  $(x_0, y_0)$ , and that  $O$  is the optical axis of the optical detecting system.

Assuming that the illumination is uniform and of unit-intensity, the aperture function for the arbitrarily positioned entrance pupil may be expressed as

$$F(x, y) = \theta(x, y) \exp[i\phi(x, y)], \quad (1)$$

where  $(x, y)$  is the position of the aperture in the entrance plane,  $\theta(x, y)$  is the transmission function, and  $\phi(x, y)$  is the phase function. The aperture function is given by

$$\theta(x, y) = \begin{cases} 1 & x_0 - a \leq x \leq x_0 + a; -b \leq y \leq y_0 + b \\ 0 & \text{otherwise} \end{cases}. \quad (2)$$

\*Address all correspondence to: Liao Zhou, E-mail: ioelz@163.com

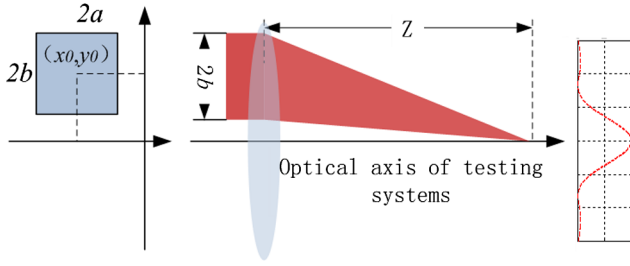


**Fig. 1** Schematic of rectangular aperture with arbitrary position of pupil and the testing systems.

According to the theory of Fourier optics, the point-spread function (PSF) of the aperture can be expressed as

$$\begin{aligned}
 \text{PSF}(\zeta, \eta) &= \left| \iint F(x, y) \exp \left[ i \frac{2\pi}{\lambda z} (x\zeta + y\eta) \right] \right|^2 \\
 &= A_k \left| \int_{x_0-a}^{x_0+a} \int_{y_0-b}^{y_0+b} \iint \exp \left[ i \frac{2\pi}{\lambda z} (x\zeta + y\eta) \right] dx dy \right|^2 \\
 &= A_k \left| \exp \left[ i \frac{2\pi}{\lambda z} (x_0\zeta + y_0\eta) \right] \right|^2 \\
 &\quad \times \left| \int_{x_0-a}^{x_0+a} \int_{y_0-b}^{y_0+b} \exp \left\{ i \frac{2\pi}{\lambda z} [(x-x_0)\zeta + (y-y_0)\eta] \right\} dx dy \right|^2 \\
 &= A_k \sin^2 c^2 \left( \frac{2\pi a \zeta}{\lambda z} \right) \sin^2 c^2 \left( \frac{2\pi b \eta}{\lambda z} \right), \quad (3)
 \end{aligned}$$

where  $(\zeta, \eta)$  is the position vector in the image plane,  $\lambda$  is the wavelength,  $z$  is the focal distance, and  $A_k$  is a coefficient.

In Eq. (3), for the diffraction image of a rectangular aperture with arbitrary position, the intensity distribution is axially symmetric with respect to the testing optical system, and the central maximum of the diffraction image lies on the optical axis of the testing system. That is to say, if the segmented primary mirror is cofocused (without tip-tilt error), the pupil's diffraction image of an arbitrary segmented mirror lies on the optical axis of the testing system. In this way, we select the cofocused segmented mirror as a reference plane, and the central maximum of its diffraction image on the testing optical system as a calibration point. The tip-tilt error and the piston error of other segmented mirrors can subsequently be detected based on the calibration point.

When the tip-tilt error exists in the segmented mirror, the tilt angles of the  $x$ - and  $y$ -axes are  $(t_x, t_y)$ , and the phase function of the pupil is given by

$$\phi(x, y) = t_x x + t_y y. \quad (4)$$

According to theory of Fourier optics, the tip-tilt error of the phase function will produce a frequency shift in the PSF. Substituting Eq. (4) into Eq. (3), we can express the PSF as

$$\text{PSF}(\zeta, \eta) = A_k \sin^2 c^2 \left( \frac{2\pi a (\zeta + \Delta\zeta)}{\lambda z} \right) \sin^2 c^2 \left( \frac{2\pi b (\eta + \Delta\eta)}{\lambda z} \right). \quad (5)$$

In this equation, the frequency shift of the PSF,  $(\Delta\zeta = t_x z, \Delta\eta = t_y z)$ , is defined only by the tip-tilt angle  $(t_x, t_y)$  and the focal distance  $z$ . If the distance between the optical axis and the central maximum of the diffraction image is detected, we can obtain the tip-tilt error of entrance pupil.

From Eqs. (3) and (5), we see that if tip-tilt error exists in the phase function, then the center of the diffraction image of the aperture deviates from the ideal optical axis (i.e., the calibration points). If the tip-tilt error of the pupil is equal to zero—i.e., if the segmented mirror is focused—then the center of the diffraction image of a single segmented mirror lies on the ideal optical axis. Therefore, by detecting the distance between the center of the diffraction image of a single segmented mirror and the testing optical axis, the tip-tilt error of that single segmented mirror can be obtained.

## 2.2 Point-Spread Function for Two Adjacent Rectangular Apertures with Piston Error

Two rectangular apertures with piston error are shown in Fig. 2. They are identical in size, with a width of  $a$  and a height of  $2a$ . The central points of the apertures lie at  $(\pm d/2, 0)$ , and the distance between the centers of the two apertures is  $d$  (where  $d \geq a$ ). The step (piston error) of the two apertures is  $\delta$ . We select an aperture as a reference mirror ( $\delta = 0$ ), and the center maximum of the diffraction image of the reference aperture as a calibration point. The piston error of the other aperture is then  $\delta$ .

At this stage, we can write the transmission function  $\theta(x, y)$  of the two apertures as

$$\theta(x, y) = \begin{cases} 1 & (\mp d - a)/2 \leq x \leq (\mp d + a)/2; -a \leq y \leq a \\ 0 & \text{otherwise} \end{cases}. \quad (6)$$

Additionally, we can express the phase function  $\phi(x, y)$  as

$$\phi(x, y) = \begin{cases} \delta x \geq 0 \\ 0 & x < 0 \end{cases}. \quad (7)$$

By substituting Eqs. (6) and (7) into Eq. (3), we can express the PSF as

$$\begin{aligned}
 \text{PSF}(\zeta, \eta) &= A_k \frac{1}{4} \left| \exp \left[ i \frac{2\pi}{\lambda z} \left( \frac{-d}{2} \zeta + 0\eta \right) \right] \int_{-a}^0 \int_{-a}^a \exp \left\{ i \frac{2\pi}{\lambda z} [(x-x_j)\zeta + (y-y_j)\eta] \right\} dx dy \right. \\
 &\quad \left. + \exp \left[ i \frac{2\pi}{\lambda z} \left( \frac{d}{2} \zeta + 0\eta \right) \right] \int_0^a \int_{-a}^a \exp \left\{ i \frac{2\pi}{\lambda z} [(x-x_j)\zeta + (y-y_j)\eta] + i\delta \right\} dx dy \right|^2 \\
 &= A_k \frac{1}{4} \left| \left\{ \exp \left[ i \frac{2\pi}{\lambda z} \left( \frac{-d}{2} \zeta \right) \right] + \exp \left( i \frac{2\pi}{\lambda z} \frac{d}{2} \zeta + i\delta \right) \right\} \sin c \left( \frac{\pi a \zeta}{\lambda z} \right) \sin c \left( \frac{2\pi a \eta}{\lambda z} \right) \right|^2 \\
 &= A_k \left[ 2 + 2 \cos \left( \frac{2\pi d \zeta}{\lambda z} + \delta \right) \right] \sin^2 c^2 \left( \frac{\pi a \zeta}{\lambda z} \right) \sin^2 c^2 \left( \frac{2\pi a \eta}{\lambda z} \right) \\
 &= A_k \cos^2 \left( \frac{\pi d \zeta}{\lambda z} + \frac{\delta}{2} \right) \sin^2 c^2 \left( \frac{\pi a \zeta}{\lambda z} \right) \sin^2 c^2 \left( \frac{2\pi a \eta}{\lambda z} \right). \quad (8)
 \end{aligned}$$

This equation is similar in form to that of Young's double-slit interference. The function is represented as the product of two factors: the interference of two apertures with piston error ( $\delta$ ), and the PSF of an individual rectangular aperture. When the relation between the calibration points and the center maximum of the inference image (with piston error) is obtained, the piston error can be calculated by measuring the coordinates of the center maximum of the interference image. Because the partial derivative is equal to zero at the function's extreme value point, if the partial derivative of Eq. (8) is calculated, the center points of the diffraction image can be easily obtained. Equation (8) is separable variable. The function is symmetrical in the  $y$ -direction; the center points of the diffraction image only change as the piston error ( $\delta$ ) changes in the  $x$ -direction; therefore, only the partial derivative with respect to  $x$  is required. However, it is difficult to differentiate Eq. (8) directly, so the Taylor expansion is required. Accordingly, we can express Eq. (8) as

$$\begin{aligned} \text{PSF}(\zeta, \eta) &= A_k \cos^2\left(\frac{\pi d \zeta}{\lambda z} + \frac{\delta}{2}\right) \sin^2\left(\frac{\pi a \zeta}{\lambda z}\right) \sin^2\left(\frac{2\pi a \eta}{\lambda z}\right) \\ &= \left[1 + \cos\left(\frac{2\pi d \zeta}{\lambda z} + \delta\right)\right] \frac{1}{\left(\frac{\pi a \zeta}{\lambda z}\right)^2} \left[1 - \cos\left(\frac{2\pi a \zeta}{\lambda z}\right)\right] \\ &\quad \times \sin^2\left(\frac{2\pi a \eta}{\lambda z}\right), \end{aligned} \quad (9)$$

where  $k_d = \pi d \zeta / \lambda z$  and  $k_a = \pi a \zeta / \lambda z$ . The function can then be expanded as a Taylor series of the variable  $\zeta$ :

$$\begin{aligned} F_\zeta &= \frac{1}{k_a^2} [1 + \cos(2k_d + \delta)][1 - \cos(2k_a)] \\ &= \frac{1}{k_a^2} \left(2 - \frac{(2k_d + \delta)^2}{2} + \frac{(2k_d + \delta)^4}{24} + \dots\right) \\ &\quad \times \left(1 - 1 + \frac{(2k_a)^2}{2} - \frac{(2k_a)^4}{24} + \dots\right) \\ &= \frac{1}{k_a^2} \left(2 - \frac{(2k_d + \delta)^2}{2} + \frac{(2k_d + \delta)^4}{24} + \dots\right) \left(2k_a^2 - \frac{2k_a^4}{3} + \dots\right) \end{aligned} \quad (10)$$

By simplifying the function and neglecting the high-order terms, we obtain:

$$F_\zeta = 4 - \frac{4}{3} k_a^2 - (2k_d + \delta)^2 \left(2 - \frac{2}{3} k_a^2\right). \quad (11)$$

The derivative is equal to zero at the function's maximum point:

$$\frac{dF_\zeta}{d\zeta} = 0. \quad (12)$$

By simplifying the function, we derive the analytical expression of relations between the calibration points and the central maximum of the interference image with piston error:

$$\zeta = \frac{3\lambda z d}{3d^2 + a^2} \delta. \quad (13)$$

If there is no gap between the two rectangular apertures in Fig. 2 (i.e.,  $a = d$ ), then Eq. (13) can be expressed as

$$\zeta = \frac{3\lambda z \delta}{4a}. \quad (14)$$

From Eqs. (13) and (14), we can see that the relationship between the piston error  $\delta$  and the coordinates of the interference image peak  $\zeta$  is linear. Moreover, the linear relationship is determined by the wavelength  $\lambda$ , the focal length  $z$ , the width of the aperture  $a$ , and the distance  $d$  between the centers of the two rectangular apertures; the relationship does not depend on the distance between the aperture and the edge of the segmented mirror. The piston error of the segmented mirror can be accurately measured if the position of the interference image peak can be effectively detected. Therefore, it is unnecessary to accurately measure the distance between the aperture and the edge of the segmented mirror, and the edge effects of the segmented mirrors can be avoided by increasing  $d$ .

### 2.3 Calculating the Center of the Diffraction Image

Because the aperture is axially symmetric about the  $x$ - and  $y$ -axes, the distribution of the diffraction image of the aperture is also axially symmetric about the  $x$ - and  $y$ -axes. Thus, the central maximum of the interference image is located at the centroid position of the image, and can be obtained by the centroid algorithm:

$$\begin{aligned} x_c &= \frac{\sum_{i=1}^m \sum_{j=1}^n I_{ij} x_i}{\sum_{i=1}^m \sum_{j=1}^n I_{ij}} \\ y_c &= \frac{\sum_{i=1}^m \sum_{j=1}^n I_{ij} y_i}{\sum_{i=1}^m \sum_{j=1}^n I_{ij}} \end{aligned} \quad (15)$$

### 3 Example of Numerical Simulation

In order to evaluate the proposal, numerical simulations of the above theoretical equations were carried out. The parameters used were as follows:  $\lambda = 0.55 \mu\text{m}$ ,  $a = 25 \text{ mm}$ ,  $d = 30 \text{ mm}$ , and  $z = 3000 \text{ mm}$ . These parameters were substituted into Eqs. (8) and (13), and the results are shown in Fig. 3. The straight line with rectangular frames in Fig. 3 displays the simulation results from Eq. (8), whereas the straight line with points displays the theoretical calculation results from Eq. (13). From the figures, we can see that the numerical simulation results are consistent with the theoretical results. With piston errors lower than  $\lambda/2$  (because of the

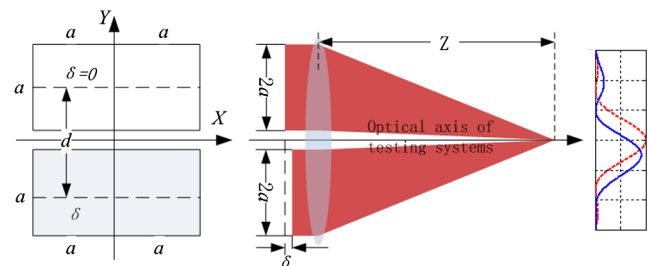


**Fig. 2** Schematic of two adjacent rectangle apertures with piston error and the testing systems.

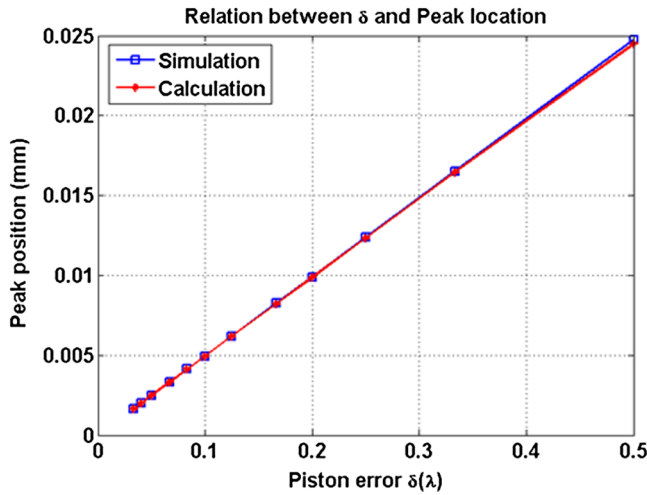


Fig. 3 Results of numerical simulation.

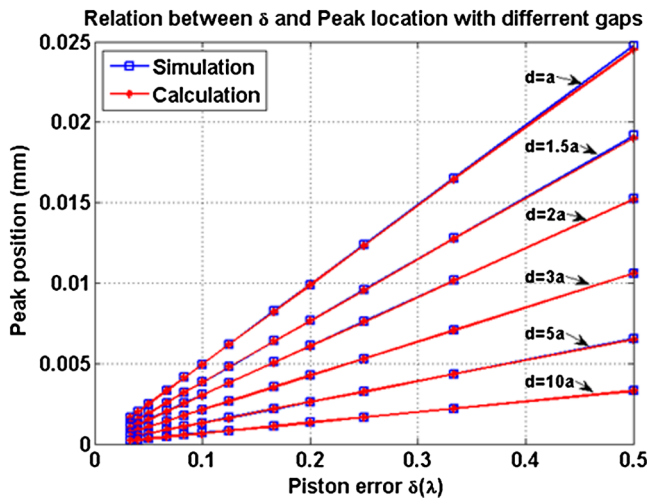


Fig.4 Simulation results for the different aperture gaps.

reflecting action of the mirror, the wavefront error is less than  $\lambda$ , the relationship between the piston error and the distance of the optical axis for the interference image peak is linear.

Figure 4 shows the relationship between the interference image peak position ( $\zeta$ ) and the piston error ( $\delta$ ) with different gaps in the aperture ( $d$ ). We can see that with an increase in the gap between two apertures, their position sensitivity decreases, whereas the detecting difficulty increases. This can be explained by the fact that the parameter  $d$  affects the interference term in such a way that the width of the interference image will decrease as a result of an increase in  $d$ . Therefore, the detection of the piston error of segmented mirrors requires comprehensive consideration and a detailed

analysis of the focal length of the testing system, the aperture size of the pupil, and the pixel size of the detecting camera.

#### 4 Conclusions

From these investigations, we conclude that the rectangular aperture with an arbitrarily positioned entrance pupil will image at the optical axis of the testing system with a symmetric diffraction shape. Moreover, the image is symmetric about the optical axis of the testing system, and thus the center of the image can be calibrated as a reference center. The relationship between the interference peak position and piston errors of two adjacent rectangular apertures (within half a wavelength of each other) is linear. By measuring the interference image peak position, the piston and tilt errors of the segmented mirrors can be quickly obtained with high accuracy. The theoretical equations that support these claims are corroborated to a high degree of accuracy by numerical simulations.

#### References

1. G. A. Chanan, J. E. Nelson, and T. S. Mast, "Segmented alignment for the Keck telescope primary mirror," *Proc. SPIE* **628**, 466–470 (1986).
2. D. C. Redding et al., "Wavefront sensing and control for large space optics," *Proc. IEEE Aerospace Conf.* **4**, 1729–1744 (2003).
3. G. Chanan et al., "Phasing the mirror segments of the Keck telescopes: the broadband phasing algorithm," *Appl. Opt.* **37**(1), 140–155 (1998).
4. G. Chanan et al., "Phasing the mirror segments of the Keck telescopes II: the narrow-band phasing algorithm," *Appl. Opt.* **39**(25), 4706–4714 (2000).
5. F. Shi et al., "Experimental verification of dispersed fringe sensing as a segment phasing technique using the Keck telescope," *Appl. Opt.* **43**(23), 4474–4481 (2004).
6. G. Chanan et al., "Phase discontinuity sensing: a method for phasing segmented mirrors in the infrared," *Appl. Opt.* **38**(4), 704–713 (1999).
7. Q. Dan-dan et al., "New method for detecting the piston of segmented mirrors: a modification of the peak ratio technique," *Proc. SPIE* **6624**, 66240N (2007).
8. Q. Dan-dan, Z. Yue-jin, and R. Yun, "Technique of detecting the piston of segmented mirrors with high accuracy based on diffraction theory," *Infrared Laser Eng.* **39**(3), 537–565 (2010).
9. R. Diaz-Uribe and A. Jiménez-Hernández, "Phase measurement for segmented optics with 1D diffraction images," *Opt. Express* **12**(7), 1192–1204 (2004).

**Liao Zhou** is an assistant researcher at the Institute of Optics and Electronics, Chinese Academy of Sciences. He received his BS and MS degrees in physics from Shandong University and Institute of Optics and Electronics in 2000 and 2003, respectively. His current research interests include adaptive optical, optical testing, and opto-mechanical systems.

**Qiu Qi** is a professor at the University of Electronic Science and Technology of China. He received his BS and MS degrees from Huazhong University of Science and Technology and University of Electronic Science and Technology of China, in 1985 and 1987, respectively. His current research interests is in the field of optical fiber communications.

**Xian Hao** is a researcher at the Institute of Optics and electronics, Chinese Academy of Sciences. He received his BS degree from Beijing Institute of Technology in 1990. His current research interests include adaptive optical, large aperture telescope, and opto-mechanical systems.